A&A 424, 347–354 (2004)
DOI: 10.1051/0004-6361:20040427
© ESO 2004

Astronomy & Astrophysics

Temperature dependence of the Lyman α line wings in cool hydrogen-rich white dwarf atmospheres. Application to ZZ Ceti white dwarf spectra

N. F. Allard[1,2], J. F. Kielkopf[3], and B. Loeillet[1]

[1] Institut d'Astrophysique de Paris, CNRS, 98 bis boulevard Arago, 75014 Paris, France
e-mail: allard@iap.fr
[2] Observatoire de Paris-Meudon, LERMA, 92195 Meudon Principal Cedex, France
[3] Department of Physics, University of Louisville, Louisville, KY 40292, USA

Received 11 March 2004 / Accepted 29 April 2004

Abstract. Theoretical Lyman α absorption profiles show a significant dependence on temperature of the H_2 satellite at 1600 Å, whereas the H_2^+ satellite at 1400 Å remains unchanged. The use of opacities calculated with different approximations concerning the electric dipole transition moment (constant, dependent on interatomic distance, and modulated by the Boltzmann factor) lead to very different synthetic absorption spectra. Our new Lyman α profiles over the ZZ Ceti range of temperatures have been used to synthesize theoretical spectra which compare very well to existing *HST* spectra.

Key words. line: profiles – stars: atmospheres – stars: white dwarfs – ultraviolet: stars

1. Introduction

In Allard et al. (1999) we derived a classical path expression for a pressure-broadened atomic spectral line shape which allows for an electric dipole moment that is dependent on the position of perturbers. The theory was applied to the atomic hydrogen Lyman lines broadened by collisions with neutral and ionized atomic hydrogen. The far wings of the Lyman series lines exhibit line satellites, enhancements that may be associated with quasi-molecular states of H_2 and H_2^+. We showed that the strengths of these features depend on the values of the electric dipole moments at the internuclear separations responsible for the satellites. Profiles were computed with and without spatial dependence of the dipole moment, and were compared with astronomical and laboratory observations. We demonstrated that the dependence of the electric dipole transition moment on interatomic separation is an important factor which cannot be neglected (Koester et al. 1998; Allard et al. 1998a). A major improvement to this work discussed in detail here is to take into account the Boltzmann factor in absorption, especially in stellar atmospheres for temperatures less than 15 000 K.

We present in Sect. 2 our new calculations of Lyman α absorption profiles, a study of the influence of the temperature on the line wings and satellites, and a comparison of profiles calculated in the different dipole approximations. These results show that the incorporation of the new profiles including a Boltzmann factor into white dwarf model atmospheres leads to more accurate synthetic spectra.

In Sect. 3 we compare a few available Hubble Space Telescope (*HST*) observations of ZZ Ceti white dwarfs to our synthetic spectra. Through these comparisons, we show that the new profiles give an excellent fit to the H_2 satellite at 1600 Å, and to the region above it. A remaining discrepancy in the H_2^+ satellite region around 1400 Å is attributed to the lack of a complete description of contributions from electron collisions to the Lyman α wing.

2. Theoretical line profiles

2.1. General expression for the spectrum

A unified theory of spectral line broadening has been developed to calculate neutral atom spectra given the interaction potentials, and radiative transition moments for relevant states of the radiating atom perturbed by collisions with other atoms. A detailed description of our unified theory of the shape of the Lyman series lines has been given by Allard et al. (1994, 1999).

The spectral line is given as the Fourier Transform of a correlation function.

$$F_\nu(\Delta\nu) = \boldsymbol{FT}\left[\exp\left(ng(s)\right)\right]. \quad (1)$$

The Fourier Transform is taken such that $F_\nu(\Delta\nu)$ is normalized to unity when integrated over all frequencies, and $\Delta\nu$ is measured relative to the unperturbed line.

Article published by EDP Sciences and available at http://www.aanda.org or http://dx.doi.org/10.1051/0004-6361:20040427

For a transition $\alpha = (i, f)$ from initial state i to final state f, we have

$$g_\alpha(s) = \frac{1}{\sum_{e,e'}{}^{(\alpha)} |d_{ee'}|^2} \sum_{e,e'}{}^{(\alpha)} \int_0^{+\infty} 2\pi\rho \mathrm{d}\rho \int_{-\infty}^{+\infty} \mathrm{d}x\, \tilde{d}_{ee'}[\,R(0)\,] \times \left[\mathrm{e}^{\frac{i}{\hbar}\int_0^s \mathrm{d}t\, V_{e'e}[\,R(t)\,]}\, \tilde{d}^*_{ee'}[\,R(s)\,] - \tilde{d}_{ee'}[\,R(0)\,] \right]. \quad (2)$$

The e and e' label the energy surfaces on which the interacting atoms approach the initial and final atomic states of the transition as $R \to \infty$ (R denotes the internuclear distance between the radiator and the perturber). The asymptotic initial and final state energies are E_i^∞ and E_f^∞, such that $E_e(R) \to E_\mathrm{i}^\infty$ as $R \to \infty$.

The total line strength of the transition is $\sum_{e,e'} |d_{ee'}|^2$. The radiative electric dipole transition moment of each component of the line depends on R, and changes during the collision. We define $\tilde{d}_{ee'}(R(t))$ as a *modulated* dipole (Allard et al. 1999)

$$D(R) = \tilde{d}_{ee'}[R(t)] = d_{ee'}[R(t)]\mathrm{e}^{-\frac{V_e[R(t)]}{2kT}}, \quad (3)$$

where the potential energy for the initial state is

$$V_e(R) = E_e(R) - E_e^\infty. \quad (4)$$

The difference potential energy $\Delta V(R)$ for a transition ee' is

$$\Delta V(R) = V_{e'e}(R) = V_{e'}(R) - V_e(R). \quad (5)$$

We neglect the influence of the potentials $V_e(R)$ and $V_{e'}(R)$ on the perturber trajectories, which remain straight lines. At time t from the point of closest approach for a rectilinear classical path we have

$$R(t) = \left[\rho^2 + (x + vt)^2\right]^{1/2}, \quad (6)$$

where ρ is the impact parameter of the perturber trajectory, v is the relative velocity, and x is the position of the perturber along its trajectory. The Boltzmann factor $\mathrm{e}^{-\frac{V_e(R)}{2kT}}$ appears because the perturbing atoms or ions are in thermal equilibrium with the radiating atom which affects the probability of finding them initially at a given R. This treatment results in a sensitive temperature dependence of the Lyman series line wing profiles. We had to use dipole moments modulated by the Boltzmann factor in the comparison of emission spectra of Lyman α (Kielkopf & Allard 1998) and Balmer α (Kielkopf et al. 2002) measured in laboratory, and in alkali line profiles used for the modeling of brown dwarf spectra (Allard et al. 2003).

2.2. Application to the Lyman α profile

As shown in Eq. (2) the fundamental data are $V_{e'e}(R)$, the difference potential for the transition, and $\vec{d}_{ee'}$, the electric dipole moment. The adiabatic interaction of a neutral hydrogen atom with a proton or another neutral hydrogen atom is described by potential energies $V_e(R)$ for each electronic state of the H_2^+ or H_2 molecule. Our calculations are based on accurate theoretical H_2^+ and H_2 molecular potentials of Madsen & Peek (1971) for H–H^+ collisions and of Detmer et al. (1998) and Schmelcher (2000) for H–H collisions. Dipole transition moments have been calculated by Ramaker & Peek (1972) and Spielfiedel (2003) respectively for H_2^+ and H_2.

Because the shapes of the ground state potentials X $^1\Sigma_g^+$ of H_2 and $2p\,\sigma_u$ of H_2^+ are very flat as $R \to \infty$, we did not investigate the effect of the Boltzmann factor on the absorption spectra of Lyman lines in previous work. However, to model the H–H collision-induced (CI) satellites due to the B$''\bar{\mathrm{B}}$ $^1\Sigma_u^+$ – X $^1\Sigma_g^+$ transition of H_2 in the Lyman β profile requires the most accurate determination possible of the short wavelength (blue) wing of Lyman α (Allard et al. 2004a). It is dominated by satellites due to H–H^+ collisions (Allard et al. 2000) and contributions from collisions with electrons. The appearance or non-appearance of the CI satellite at 1150 Å is very sensitive to the strength of the blue wing of Lyman α, and we have shown in Allard et al. (2000) that the density of neutral hydrogen must be at least a factor of five greater than the density of protons and electrons for the 1150 Å CI satellite of Lyman β to be distinguishable.

The blue wing H_2^+ satellites of Lyman α are formed at small internuclear distances (Allard et al. 1994). At these distances the H_2^+ potential of the ground state is *not* flat, but has a short range potential barrier. The effect of the Boltzmann factor is then not negligible and it must be included to take into proper account all of the combined contributions of the Lyman α and β wings of H perturbed simultaneously by neutral and ionized hydrogen.

The CI absorption depends strongly on the internuclear separation during the collision and produces a broad spectral feature with a characteristic width of the order of the inverse of the duration of the close collision. The CI hydrogen satellite at 1150 Å differs from other satellite features previously detected in that it depends on a large increase in the transition probability when the interacting atoms move through the difference energy minimum of the potential surface that produces radiation at 1150 Å. This dependence on transition probability spatially selects a small range of interatomic separations from which the spectral feature may arise, and generates a unique dependence of the feature on density and temperature. The CI satellite is presented in Fig. 1. The blue wing of the satellite itself, which extends until the 1080 Å satellite, is very temperature-dependent. The oscillations which appear are due to interference effects (Royer 1971; Sando & Wormhoudt 1973) and depend on the relative velocity and therefore on temperature. At 12 000 K the maxima of these oscillations are at 1099 and 1115 Å and are visible in the synthetic spectrum presented in Fig. 3.

The spectrum between 1080 and 1215 Å is then highly temperature dependent because of the overlap of the blue wing of Lyman α due to H_2^+ satellites with the far red wing of Lyman β extending from 1080 to 1180 Å dominated by its CI H_2 satellite at 1150 Å (Allard et al. 2000).

In the Lyman α far red wing the H_2 satellite situated at 1600 Å is formed at an internuclear distance (2.2 Å) where the potential of the ground state starts to increase with decreasing R. The effect of modulation of the dipole moment by the Boltzmann factor is then very important especially in the

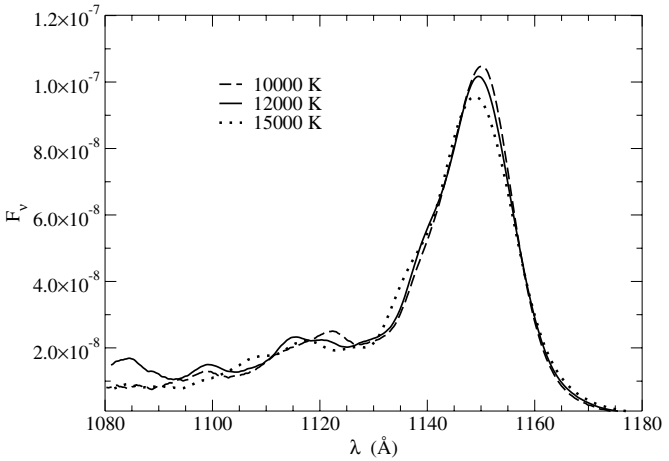

Fig. 1. Variation of the CI satellite at 1150 Å with T. The neutral density $n_{\rm H}$ is 1×10^{18} cm^{-3}.

ZZ Ceti range of temperatures, whereas it is not important for the other Lyman series satellites formed at a larger internuclear distance (Allard et al. 1994, 1998a, 2000).

To point out the importance of the temperature we have displayed in Fig. 2a the variation of the modulated radiative dipole moment for the B-X transition which gives rise to the 1600 Å satellite. The dipole moment changes significantly in close collisions from its aymptotic value for the unperturbed atom. Moreover, Fig. 2a shows that when the temperature is reduced there is a large increase in the amplitude of the modulated dipole moment compared to the original dipole transition moment $d_{ee'}(R)$(T_∞ in Fig. 2a) calculated by Spielfiedel (2002).

We show in Fig. 2b the influence of temperature on the amplitude of the 1600 Å satellite. The effect of temperature becomes important mainly when the temperature is less than 15 000 K. The line satellites have a strong blanketing effect and have to be included for the determination of the structure of the atmosphere (Koester & Allard 1993). It is consequently necessary to use opacities calculated using the dipole moment modulated by the Boltzmann factor in absorption to get a correct temperature profile for the model. The synthetic spectra of white dwarfs for $T < 15\,000$ K are very sensitive to the effect of temperature on the Lyman α region profile. We show in Fig. 3 a comparison of synthetic spectra obtained when using the different approximations for the dipole moment. The total Lyman β profile has been calculated only with variable dipole moment as the CI satellite, by definition, would not exist in the constant dipole approximation. The line satellites at 1060 and 1080 Å, first identified as H_2^+ quasi-molecular satellites of Lyman β by Koester et al. (1996), are formed at large internuclear distance and are not temperature-dependent.

3. Application to ZZ Ceti white dwarfs

We will restrict our study to ZZ Ceti white dwarfs, because of very good *HST* spectra which allow a precise comparison with synthetic spectra, although this temperature effect would be even more important for cooler stars like λ Bootis or metal-deficient horizontal branch stars which present the Lyman α H_2 satellite at 1600 Å (Holweger et al. 1994; Allard et al. 1998b).

ZZ Ceti stars are variable DA white dwarfs mainly constituted of pure hydrogen. They are confined to a narrow strip centered around $T_{\rm eff} \approx 12\,000$ K. In this temperature range, the red wing of Lyman α in these objects is dominated by two broad features at 1400 and 1600 Å which were interpreted respectively as atom-proton and atom-atom absorption by Koester et al. (1985) and Nelan & Wegner (1985).

We will consider LTE model atmospheres with pure hydrogen composition that explicitly include the Lyman α and Lyman β quasi-molecular opacities. For the Lyman α and Lyman β lines we use the profiles obtained for $T_{\rm eff} = 12\,000$ K, but, in principle, profiles obtained for different temperatures should be used for the determination of the structure of the atmosphere as the temperature dependence of the line profiles is significant in the range of temperature of ZZ Ceti stars. This will be taken into account in future work.

The atmosphere models have been calculated using the program TLUSTY (Hubeny 1988; Hubeny & Lanz 1992, 1995). The resulting spectra were computed by using the spectral synthesis code SYNSPEC that incorporates the quasi-molecular satellites of Lyman lines.

The fits to the 1400 and 1600 Å features are especially sensitive to the assumed parameters for the convection efficiency which constitute the main uncertainty for the models and for the determination of atmospheric parameters. Convection is usually described within the framework of the mixing length approximation (MLT), where we used ML2/α = 0.6, parameters determined by Bergeron et al. (1995), to get consistency between ultraviolet and optical temperatures. We note that these parameters were obtained using quasi-molecular calculations of Allard et al. (1994) using the constant dipole moment approximation.

4. Comparison of observed spectra with theoretical models

Our new profiles incorporated in white dwarf model atmospheres yield synthetic spectra that predict that both H_2 and H_2^+ satellites of the Lyman α *and* Lyman β lines should be detectable roughly from 11 000 to 13 000 K (Hébrard et al. 2002). This small temperature range includes the ZZ Ceti instability strip, and in Figs. 4, 6, 7, and 8 we compare these synthetic spectra with *HST* spectra of several ZZ Ceti stars. The temperature and gravity for each synthetic spectrum shown here were determined to give visual best fit to the observed spectrum. The synthetic spectra are normalized to the *HST* spectra at 2200 Å.

With an optimal adjustment of these parameters, it is possible in each case to have a good fit to the H_2 satellite at 1600 Å and to the region beyond it, but for the same parameters there is a discrepancy in the region around 1400 Å. The models give a deeper H_2^+ satellite at 1400 Å than is observed.

The sensitivity of a synthetic spectrum to the contributions from broadening by electron collisions was tested by computing models with broadening by electrons switched off. These tests revealed that the 1400 Å region is quite sensitive to the electron-broadening profile, but the 1600 Å region is not. We conclude from this that a more accurate description of broadening by electrons than is presently available will be required to

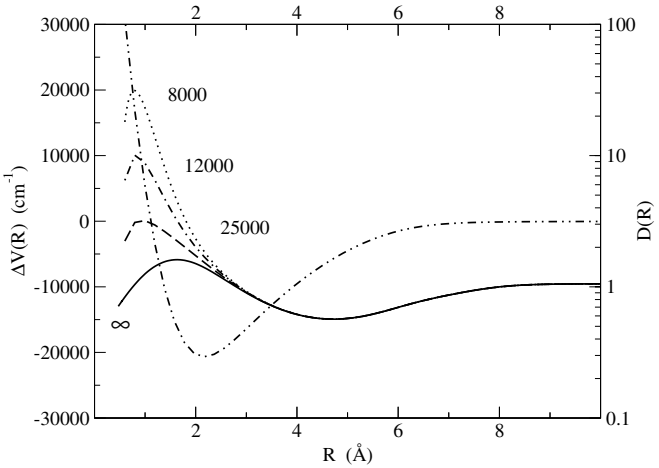

(a) Variation of the modulated radiative dipole moment and the difference potential energy for the B-X transition as a function of internuclear distance.

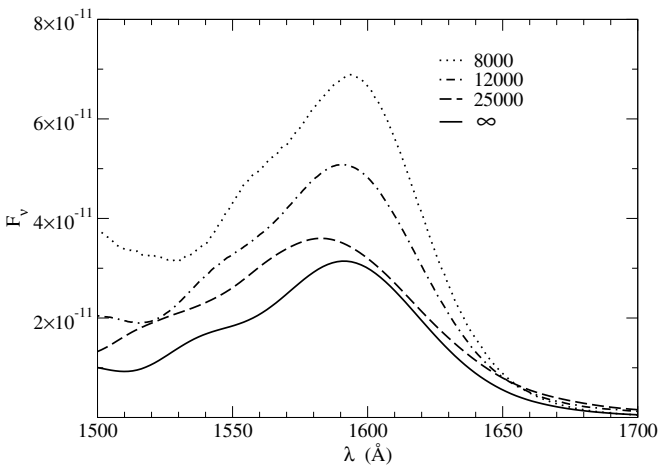

(b) The Lyman α H_2 satellite at 1600 Å. The neutral density n_H is 1×10^{16} cm^{-3}.

Fig. 2. The 1600 Å line satellite and its corresponding modulated dipole moment as a function of temperature.

improve the quality of the fit in the H_2^+ satellite region around 1400 Å. The synthetic spectrum between Lyman α and β, below the range of *HST* but accessible with the Far Ultraviolet Telescope (*FUSE*), is even more deeply affected by the electron collision contributions to the profile.

For the case of G226-29 shown in Fig. 4 we used a very high S/N spectrum (Koester, private communication) obtained using time-resolved *HST* spectra presented by Kepler et al. (2000). This comparison allows us to make a temperature and gravity determination that is compatible with a fit to the *FUSE* observation of this object (Allard et al. 2004a).

Figure 4a shows our fit to the *HST* spectrum using our adopted values for $T_{\rm eff} = 12\,040$ and $\log g = 7.93$. As pointed out by Bergeron et al. (1995), the UV spectra alone do not allow a unique solution. It is possible to fit the *HST* spectrum with higher $T_{\rm eff}$ and higher $\log g$, and the optical determination of Bergeron et al. (1995) ($T_{\rm eff} = 12460, \log g = 8.29$) also gives an excellent fit to the *HST* spectrum. Using opacities of Allard et al. (1994) and an International Ultraviolet Telescope (*IUE*) spectrum, the determination in the UV was ($T_{\rm eff} = 12270$, $\log g = 8.29$). With our new calculations for a given gravity we obtain a higher temperature because the H_2 satellite is much deeper. The determination of atmospheric parameters of G226-29 using a fit to the UV and optical spectra now leads to identical results.

While it is possible to fit the UV spectra with different pairs of atmospheric parameters, the observation of the Lyman β wing gives us an additional constraint because a compensation of increasing $\log g$ by an increasing $T_{\rm eff}$ is not possible as it was in the UV range. This is demonstrated in Fig. 4 which shows that parameters that produce nearly identical spectra above Lyman α yield distinguishably different spectra in the Lyman β red wing.

As noticed in Allard et al. (2004a) we need to divide the flux in the Lyman α range by a factor 1.3 to compare with the *FUSE* spectrum of G226-29. Figure 5 compares with *FUSE* spectrum to the synthetic spectra obtained for (12040/7.93) and (12460/8.28) respectively multiplied by 0.66 and 0.77 to get the line satellites to fit with the *FUSE* observation. The comparison seems to favor the lower temperature, lower gravity pair but, as we mentioned above, this part of the spectrum is strongly affected by electron collision contributions and we need to use a more accurate description of the electron-broadening profile to draw definitive conclusions.

The determination of the ZZ Ceti instability strip has been included in a number of recent analyses which use UV spectra together with additional constraints like parallaxes, V magnitude, or gravitational redshifts where the authors point out the difficulty of obtaining reliable parameters (Koester & Vauclair 1997; Koester & Allard 2000; Koester & Holberg 2001). The uncertainties are not restricted to the theory of convection, but include the opacities themselves. We have shown here how a simple assumption of constant transition dipole moment and a profile independent of temperature could lead to very different results for parameters derived from synthetic spectra.

Although our goal is not the determination of the atmospheric parameters, considering the remaining uncertainties with electron collision contributions to the profiles, and because we did not use additional constraints, we have summarized in Table 1 our resulting effective temperatures and gravities and compared them with those obtained by Koester & Holberg (2001) and Bergeron et al. (1995). These data show a general trend of smaller gravities with the more accurate line shape theory. For GD165 Koester & Holberg (2001) gave two solutions according to whether the constraint is done with parallax (P) or visual magnitude (V).

5. Conclusion

The contribution of electrons, protons and neutral atoms to the spectrum between 1080 and 1215 Å is complicated by the

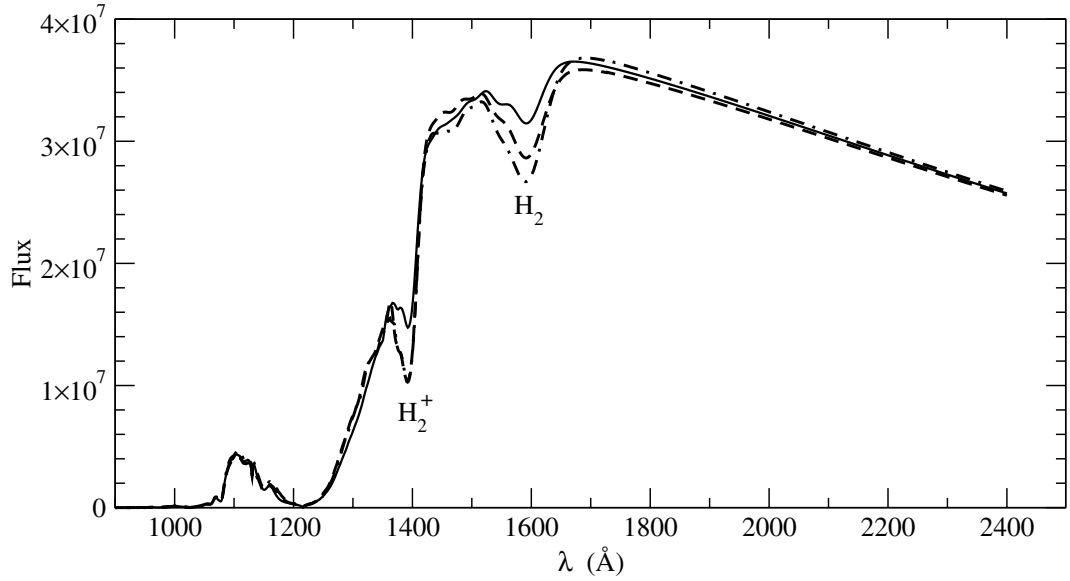

(a) Lyman α and Lyman β.

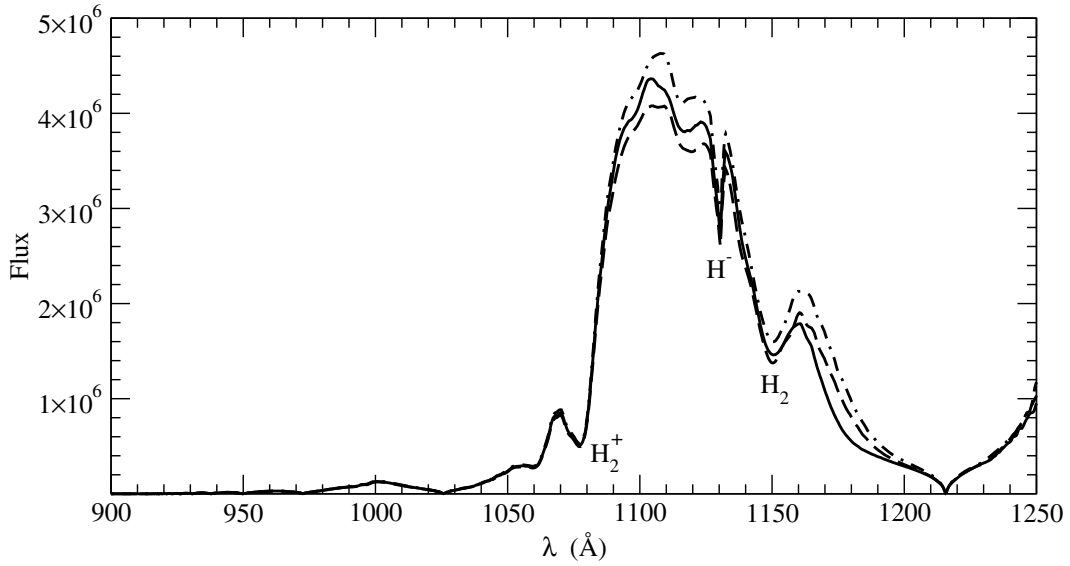

(b) Detail of the *FUSE* Lyman β region in the far ultraviolet.

Fig. 3. Comparison of theoretical absorption spectra including Lyman satellites with opacities calculated with different approximations of the dipole moments for $T_{\rm eff}$ = 12 000 K and $\log g$ = 7.9 . Solid line: constant dipole; dashed line: variable dipole; dashed dotted line: modulated dipole.

overlap of the red wing of Lyman β and the blue wing of Lyman α. This results in a very constrained model due also to the nature of the strong CI neutral satellite at 1150 Å. Because of this, we emphasize the importance of the accuracy of both the potential energies *and* the electric dipole transition moments for the line shape calculations. It is necessary to have a theory which takes into account the variation of the transition dipole moment with atomic separation to obtain reliable line profiles. Without both the accurate atomic data and the complete line shape theory it is *impossible* to determine the CI satellite since its existence is totally bound to them (Allard et al. 2000).

To conclude, we emphasize that it is important to use accurate line profiles, and to be cautious about the range of validity of the opacities which are used as pointed out in Allard et al. (2004b). Below 15 000 K it is necessary to use temperature-dependent opacities. For hotter stars with high gravity the Lyman β and Lyman γ profiles have to be evaluated in a unified line shape theory and the density expansion of the autocorrelation function in Eq. (1) we presently use (Allard et al. 1994) is no longer valid (Allard et al. 2004b). This explains the discrepancy between theoretical and observed quasi-molecular satellites in the spectra of massive white dwarfs (Dupuis et al. 2003).

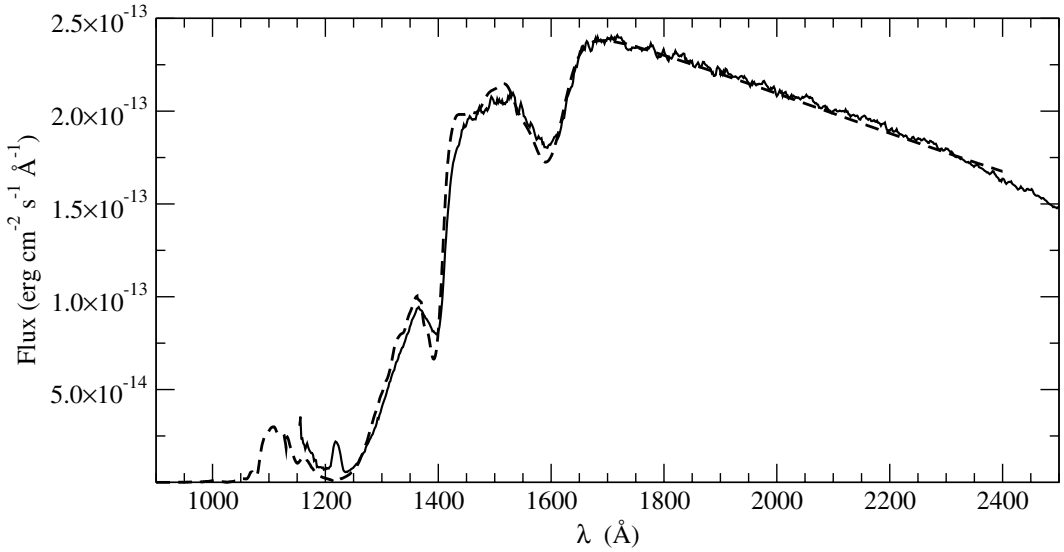

(a) G226-29 *HST* spectrum compared with a synthetic spectrum for T = 12 040 K and log g = 7.93.

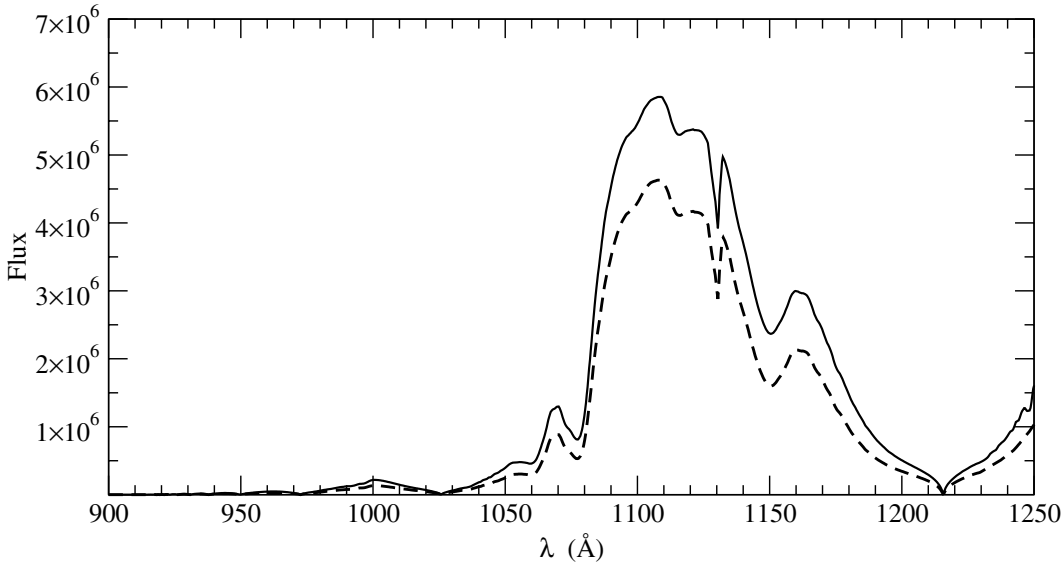

(b) Comparison of two synthetic spectra in the *FUSE* Lyman β range. Solid line: $T_{\rm eff}$ = 12 040 K log g = 7.93; dashed line: $T_{\rm eff}$ = 12 460 K log g = 8.28.

Fig. 4. Comparison of theoretical spectra for two pairs of parameters ($T_{\rm eff}$ = 12 040 K and log g = 7.93) and ($T_{\rm eff}$ = 12 460 K and log g = 8.28) in the Lyman α and Lyman β range, and the *HST* spectrum of G226-29.

Table 1. Atmospheric parameters $T_{\rm eff}$ and log g.

Name	WD	A04	KH01	B95
G226-29	1647+591	12040/7.93	12020/8.24	12460/8.29
G117-B15A	0921+354	12000/7.85	12010/7.94	11620/7.97
G185-32	1935+276	12080/7.9	11910/8.04	12130/8.05
GD165	1422+095	11970/7.65	11800/7.76 (P)	11980/8.06
			12130/8.20 (*V*)	

One improvement will be the inclusion of Lyman opacities obtained at different temperatures in the modeling of the atmosphere and in the synthesis of theoretical spectra. Nevertheless, another major and crucial improvement will be an accurate calculation of an electron-broadening profile which releases us from the use of the quasi-static approximation in the wing. We hope to achieve this in the future.

The region below 1215 Å is potentially very promising for determining atmospheric parameters provided that accurate line profile calculations of H perturbed by neutral H, H^+ and e^-

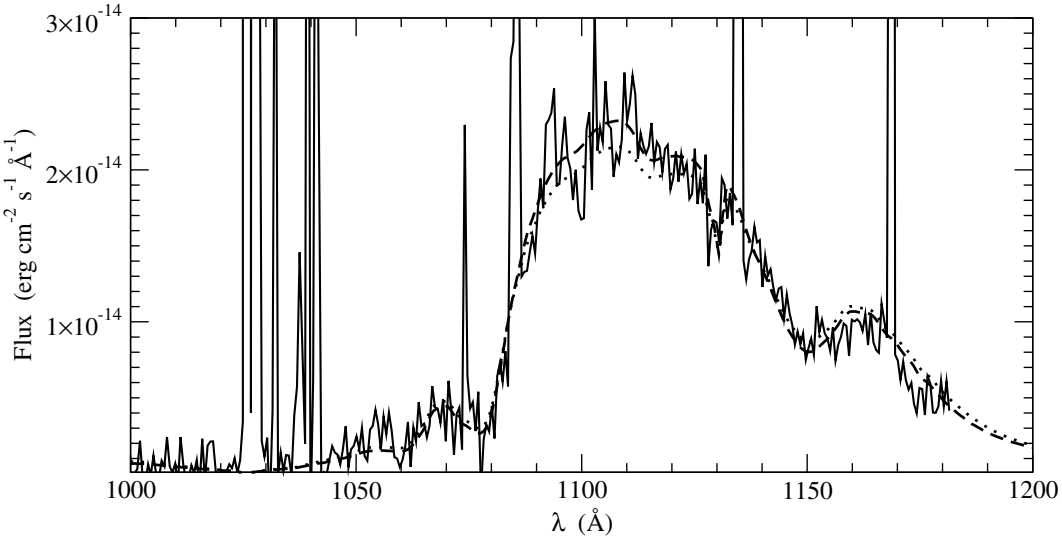

Fig. 5. Comparison of two synthetic spectra in the Lyman β range with a *FUSE* spectrum of G226-29. Dashed line: $T_{\rm eff}$ = 12 040 K and $\log g$ = 7.93; dotted line: $T_{\rm eff}$ = 12 460 K and $\log g$ = 8.28.

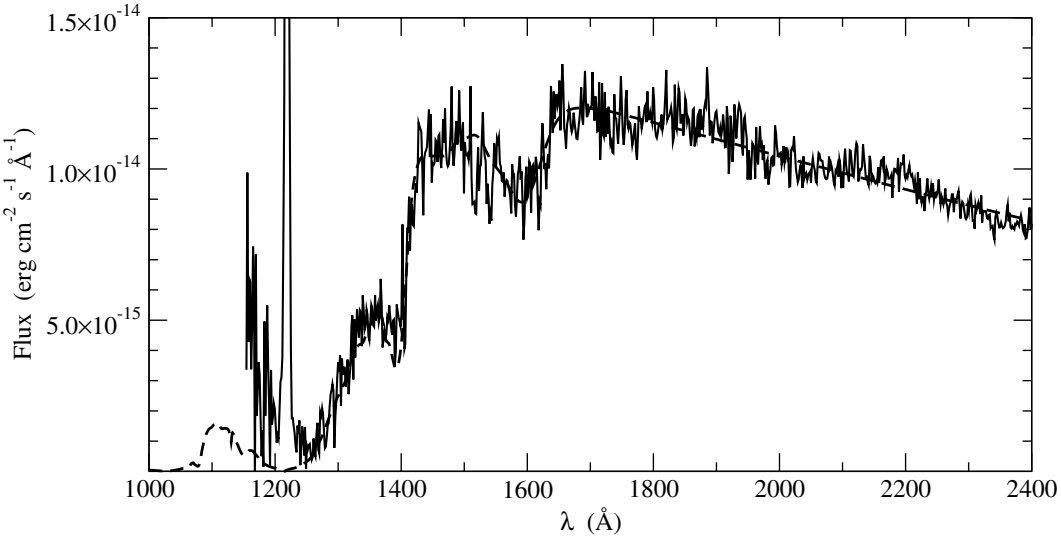

Fig. 6. *HST* spectrum of G117-B15A compared with $T_{\rm eff}$ = 12 000 K and $\log g$ = 7.85.

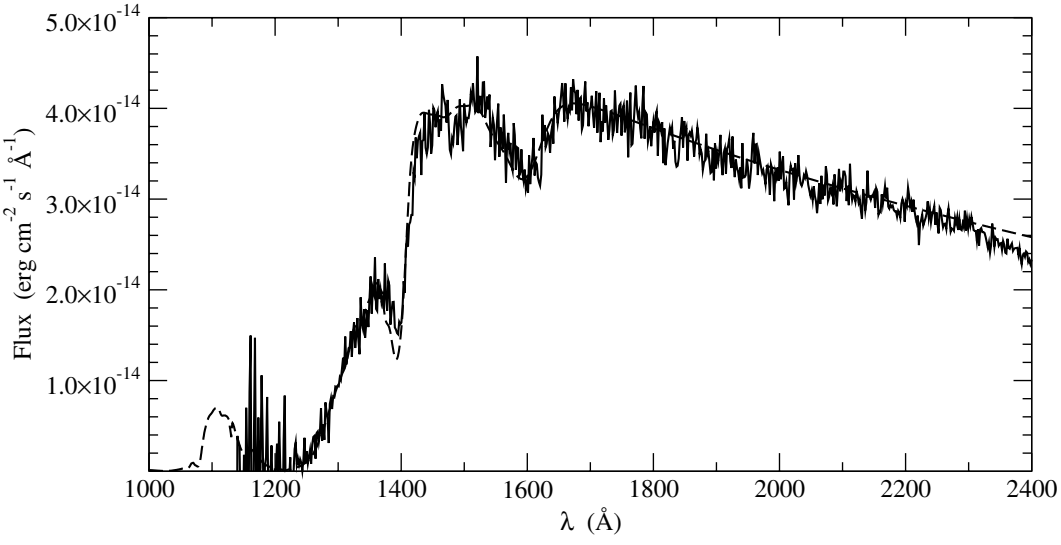

Fig. 7. *HST* spectrum of GD165 compared with $T_{\rm eff}$ = 11 970 K and $\log g$ = 7.65.

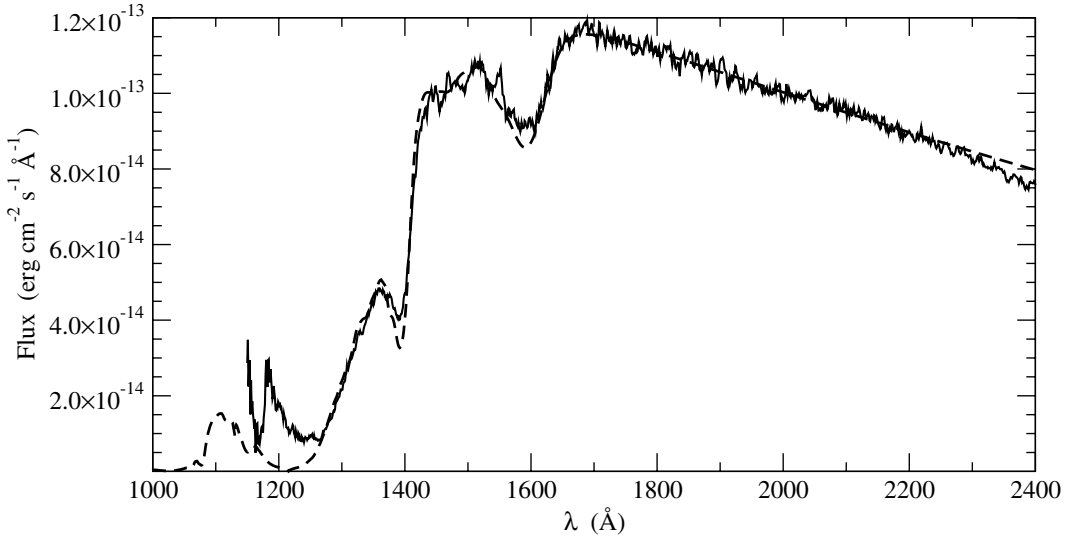

Fig. 8. *HST* spectrum of G185-32 compared with $T_{\rm eff}$ = 12 080 K and $\log g$ = 7.9.

are used together with high quality ultraviolet and far ultraviolet spectra.

Theoretical profiles can be obtained from N. F. Allard upon request.

References

Allard, N. F., Koester, D., Feautrier, N., & Spielfiedel, A. 1994, A&A, 108, 417
Allard, N. F., Kielkopf, J. F., & Feautrier, N. 1998a, A&A, 330, 782
Allard, N. F., Drira, I., Gerbaldi, M., Kielkopf, J. F., & Spielfiedel, A. 1998b, A&A, 335, 1124
Allard, N. F., Royer, A., Kielkopf, J. F., & Feautrier, N. 1999, Phys. Rev. A, 60, 1021
Allard, N. F., Kielkopf, J. F., Drira, I., & Schmelcher, P. 2000, Eur. Phys. J. D, 12, 263
Allard, N. F., Allard, F., Hauschildt, P. H., Kielkopf, J. F., & Machin, L. 2003, A&A, 411, L473
Allard, N. F., Hébrard, G., Dupuis, J., et al. 2004a, ApJ, 601, L183
Allard, N. F., Kielkopf, J. F., Hébrard, G., & Peek, J. M. 2004b, Eur. Phys. J. D, 29, 7
Bergeron, P., Wesemael, F., Lamontagne, R., et al. 1995, ApJ, 449, 258
Detmer, T., Schmelcher, P., & Cederbaum, L. S. 1998, J. Chem. Phys., 109, 9694
Dupuis, J., Chayer, P., Vennes, S., Allard, N. F., & Hébrard, G. 2003, ApJ, 598, 486
Hébrard, G., Allard, N. F., Hubeny, I., et al. 2002, A&A, 394, 647
Holweger, H., Koester, D., & Allard, N. F. 1994, A&A, 290, L21
Hubeny, I. 1988, Comp. Phys. Comm., 52, 103
Hubeny, I., & Lanz, T. 1992, A&A, 262, 501
Hubeny, I., & Lanz, T. 1995, ApJ, 439, 875
Kepler, S. O., Robinson, E. L., Koester, D., et al. 2000, ApJ, 539, 379
Kielkopf, J. F., & Allard, N. F. 1998, Phys. Rev. A, 58, 4416
Kielkopf, J. F., Allard, N. F., & Decrette, A. 2002, Eur. J. Phys. D, 18, 51
Koester, D., & Allard, N. F. 1993, in White Dwarfs: Advances in Observation and Theory, ed. M. Barstow, 237
Koester, D., & Allard, N. F. 2000, Baltic Astron., 9, 119
Koester, D., & Holberg, J. B. 2001, in 12th European Workshop on White Dwarfs, ed. J. L. Provencal, H. L. Shipman, J. MacDonald, & S. Goodchild (San Francisco: ASP), ASP Conf. Ser., 226, 299
Koester, D., & Vauclair, G. 1997, in White Dwarfs, ed. J. Isern, M. Hernanz, & E. Garcia-Berro (Dordrecht: Kluwer), 429
Koester, D., Weidemann, V., Zeidler, K. T. E. M., & Vauclair, G. 1985, A&A, 142, L5
Koester, D., Finley, D. S., Allard, N. F., Kruk, J. W., & Kimble, R. A. 1996, ApJ, 463, L93
Koester, D., Sperhake, U., Allard, N. F., Finley, D. S., & Jordan, S. 1998, A&A, 336, 276
Madsen, M. M., & Peek, J. M. 1971, Atomic Data, 2, 171
Nelan, E. P., & Wegner, G. 1985, ApJ, 289, L31
Ramaker, D. E., & Peek, J. M. 1972, J. Phys. B, 5, 2175
Royer, A. 1971, Phys. Rev. A, 43, 499
Sando, K. M., & Wormhoudt, J. G. 1973, Phys. Rev. A, 7, 1889
Schmelcher, P. 2000, private communication
Spielfiedel, A. J. 2003, Mol. Spectrosc., 217, 162